

# Generative Modeling Helps Weak Supervision (and Vice Versa)

Benedikt Boecking<sup>1</sup> Willie Neiswanger<sup>2</sup> Nicholas Roberts<sup>3</sup>  
Stefano Ermon<sup>2</sup> Frederic Sala<sup>3</sup> Artur Dubrawski<sup>1</sup>

<sup>1</sup>Carnegie Mellon University <sup>2</sup>Stanford University <sup>3</sup>University of Wisconsin

## Abstract

Many promising applications of supervised machine learning face hurdles in the acquisition of labeled data in sufficient quantity and quality, creating an expensive bottleneck. To overcome such limitations, techniques that do not depend on ground truth labels have been developed, including weak supervision and generative modeling. While these techniques would seem to be usable in concert, improving one another, how to build an interface between them is not well-understood. In this work, we propose a model fusing weak supervision and generative adversarial networks. It captures discrete variables in the data alongside the weak supervision derived label estimate. Their alignment allows for better modeling of sample-dependent accuracies of the weak supervision sources, improving the unobserved ground truth estimate. It is the first approach to enable data augmentation through weakly supervised synthetic images and pseudolabels. Additionally, its learned discrete variables can be inspected qualitatively. The model outperforms baseline weak supervision label models on a number of multiclass classification datasets, improves the quality of generated images, and further improves end-model performance through data augmentation with synthetic samples.

## 1 Introduction

How can we get the most out of data when we do not have ground truth labels? Two prominent paradigms operate in this setting. First, *weak supervision* frameworks use weak sources of training signal to estimate pseudolabels that can be used to train downstream supervised models, without needing access to any ground-truth labels (Riedel et al., 2010; Ratner et al., 2016; Dehghani et al., 2017; Lang & Poon,

2021). Second, *generative models* enable learning data distributions which can benefit downstream tasks, e.g. via data augmentation or representation learning, in particular when learning disentangled representations (Higgins et al., 2018; Locatello et al., 2019; Hu et al., 2019). Intuitively, these two paradigms should complement each other, as each can be thought of as a different approach to extracting structure from unlabeled data. However, there is no simple way to combine them.

Fusing generative models with weak supervision holds substantial promise. For example, it should yield large reductions in data acquisition costs for training complex models. Weak supervision replaces the need for manual, pointillistic annotations by applying so-called labeling functions to all of the unlabeled data, producing label estimates that can be combined into a pseudolabel on each unlabeled data point. This leaves the majority of the acquisition budget to be spent on unlabeled data, and here generative modeling can reduce the number of real-world samples to be collected. Similarly, the pseudolabels produced by weak supervision may improve generative models, reducing the need to acquire large volumes of samples to improve the generative performance. Pseudolabels may for example enable class-conditional generation of samples without access to ground truth.

The main technical challenge is to build an *interface* between the core models used in the two approaches. For example, in the generative adversarial models (GANs) (Goodfellow et al., 2014) that we focus on in this work, there is at least a generator and a discriminator, and frequently additional auxiliary models, such as those that learn to disentangle latent factors of variation (Chen et al., 2016). In weak supervision, the *label model* is the main focus. How should we connect the generator, discriminator, and the label model? It is necessary to develop an interface that correctly aligns the structures learned from the unlabeled data by the various components.

We introduce a simple but powerful interface that produces the desired model alignments, shown in Fig. 2. Our approach builds on the InfoGAN (Chen et al., 2016) gen-

<sup>1</sup>boecking@cmu.edu, awd@cmu.edu

<sup>2</sup>neiswanger@cs.stanford.edu, ermon@cs.stanford.edu

<sup>3</sup>nick11roberts@cs.wisc.edu, fred sala@cs.wisc.edu

erative model, and is also inspired by the encoder-based label model component of a recently-proposed end-to-end weak supervision framework (Cachay et al., 2021). These techniques expose structure in the data, and our approach ensures alignment between the resulting variables by building projections between them. Our fused generative and weak supervision model offers a number of benefits, including:

- **Improved weak supervision:** Replacing the conventional label model in weak supervision, we obtain better-quality pseudolabels, yielding consistent improvements in pseudolabel accuracy up to 6% over weak supervision techniques such as Snorkel (Ratner et al., 2020).
- **Improved generative modeling:** Weak supervision provides information about unobserved labels which can be used to obtain better disentangled latent variables, thus improving the model’s generative performance. Our approach improves image generation by an average of 7 FID points versus InfoGAN.
- **Data augmentation via synthetic samples:** Our trained model can generate synthetic samples to augment the dataset as well as provide label estimates for the synthetic samples (see Fig. 1), enabling further improvements of downstream classifier accuracy of up to 3.9%, even when labeling functions are unavailable for synthetic samples.

## 2 Background

As we propose to fuse weak supervision with generative modeling to the benefit of both techniques, we first provide brief background on each of these methods. A broader review of related work is presented in Section 5.

**Weak Supervision** Weak supervision methods using imperfect and partial labels (Ratner et al., 2016, 2020; Cachay et al., 2021) seek to replace hand-labeling for the construction of large training datasets. Instead, users rely on multiple weak sources that, while noisy and inaccurate, can be cheaply acquired and efficiently applied to the entire dataset to provide imperfect, partial labels. Such sources can be heuristics or rules (expressed as small programs), knowledge base lookups, off-the-shelf models, and more.

The technical challenge is to combine the source votes into a high-quality pseudolabel. This requires estimating the accuracies and dependencies between sources and using them to compute a posterior label distribution. This synthesis step is performed by the *label model*. Prior works have considered various choices for the label model, most of which only take the weak source outputs into account. A review can be found in Zhang et al. (2021, 2022). Similar to Cachay et al. (2021), our choice of label model uses both the features and weak supervision votes, producing improved modeling of source accuracies.

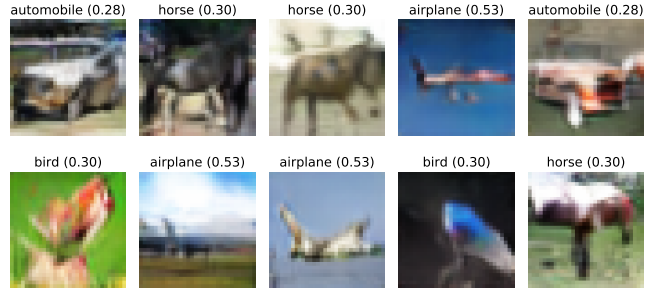


Figure 1: Synthetic images and pseudolabels generated by the proposed WSGAN, learned from weakly supervised CIFAR10. WSGAN can estimate pseudolabels for these synthetic images even without access to labeling function votes.

**Generative Models and GANs** Generative models are used to model and sample from complex distributions. Among the most popular such models are generative adversarial networks (GANs) (Goodfellow et al., 2014). GANs consist of a generator and discriminator model that play a minimax game against each other. Quantitative measures of generated image quality exist, such as the Inception Score (IS) (Salimans et al., 2016) and the Fréchet Inception Distance (FID) (Heusel et al., 2017). Despite known drawbacks (Barratt & Sharma, 2018; Borji, 2019), these measures are widely used to compare image quality. While many sophisticated variations of GANs have been proposed, our proposed approach builds off InfoGAN (Chen et al., 2016). InfoGAN adds an auxiliary inference model that helps the generative model learn disentangled representations—a set of factors of variation. We hypothesize that connecting these variables to exposed structure in the label model should yield benefits for both weak supervision and generative modeling.

## 3 The WSGAN Model

We will now establish the problem setting and describe our proposed weakly-supervised GAN (WSGAN) model, visualized in Fig. 2.

### 3.1 Problem Setting

We work with  $n$  unlabeled samples  $X \in \mathcal{X} \subseteq \mathbb{R}^d$  drawn from a distribution  $\mathcal{D}_X$ . We have two goals we want to achieve with the samples  $X$ . First, in generative modeling, we will approximate  $\mathcal{D}_X$  with a model that can be used to produce high-fidelity synthetic samples.

Second, in supervised learning, we wish to use  $X$  to predict labels  $Y \in \{1, 2, \dots, C\}$ , where  $(X, Y)$  is drawn from a distribution whose marginal distribution is  $\mathcal{D}_X$ . However, in the weak supervision setting, we do not observe  $Y$ . Instead, we observe  $m$  labeling functions that provide

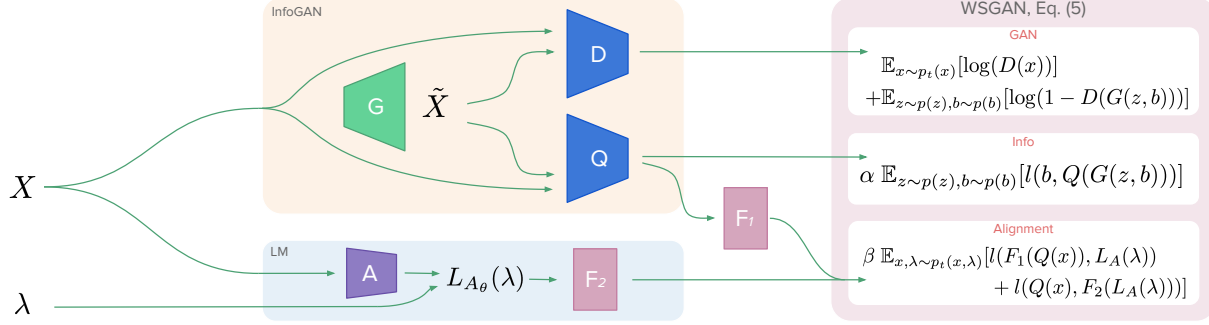


Figure 2: The proposed WSGAN architecture models discrete latent variables in  $X$  via a network  $Q$ , while the generator  $G$  continues to fool the discriminator model  $D$  with generated images  $\tilde{X}$ . Simultaneously, a label model  $L$  receives weights from an accuracy encoder  $A$  to produce an estimate of the unobserved ground truth label of  $X$  based on the observed weak supervision votes  $\lambda$ . The WSGAN model aligns this label estimate with the discrete latent variable learned by  $Q$ .

imperfect estimates of  $Y$ . These labeling functions (LFs), denoted  $\lambda_i$  for  $1 \leq i \leq m$ , vote on a sample  $x$  to produce an estimate  $\lambda_i(x) \in \{0, \dots, C\}$ , where 0 indicates abstain. The goal is to combine the  $m$  estimates into a pseudolabel  $\hat{Y}$  that can be used to train a supervised model (Ratner et al., 2016).

While weak supervision and generative modeling function over a number of domains, in this work we focus on images. Image tasks are especially challenging for weak supervision, since constructing LFs is more difficult than for, e.g., text tasks (cf. Section 5).

### 3.2 Proposed Method

To improve generative performance and the quality of the weak supervision-based pseudolabels, we propose a model that consists of a number of components. Because we wish to ensure our component models benefit each other, our architecture aims for the following characteristics:

- A generative model component that learns factors of variation from data (these could be, for example, disentangled representations or discrete structure) and exposes these externally,
- A weak supervision label model component that uses feature information to make predictions of the label anchored in the weak supervision votes, but using sample-dependent weights,
- A set of *interface* models that connect the components. Our design choices are made to satisfy those goals.

**GAN Architecture** We write  $G(x; \psi_g)$  for the generator; its goal is to learn a mapping to the image space based on input consisting of samples  $z$  from a noise distribution  $p_Z(z)$  along with a set of latent factors of variation  $b \sim p(b)$ , following the ideas introduced in Chen et al. (2016). Here, we restrict ourselves to discrete factors of variation. The output of the mapping are samples  $x$ ; these are consumed

by a discriminative model  $D(x; \psi_d)$ , which estimates the probability that a sample came from the training distribution rather than  $G$ , and outputs a scalar.

Furthermore, as in InfoGAN (Chen et al., 2016), we define an auxiliary model  $Q(x; \psi_q)$  which will learn to map from a sample  $x$  to the discrete latent code  $b$ . This model  $Q$  is used to teach the generator  $G$  disentangled, discrete representations. First, we write the standard GAN objective as:

$$\min_G \max_D V(D, G) = \mathbb{E}_{x \sim p_t(x)} [\log(D(x))] + \mathbb{E}_{z \sim p(z), b \sim p(b)} [\log(1 - D(G(z, b)))] \quad (1)$$

Next, we write the InfoGAN objective as:

$$\min_{G, Q} \max_D IV(D, G, Q) = V(D, G) + \alpha \mathbb{E}_{z \sim p(z), b \sim p(b)} [l(b, Q(G(z, b)))] \quad (2)$$

where  $l$  is an appropriate loss function, such as cross entropy, and  $\alpha$  is a hyperparameter for the InfoGAN term. This approach, presented in Chen et al. (2016), maximizes the mutual information between generated images and  $b$  while  $G$  continues to fool the discriminator  $D$ , leading to the discovery of discrete, disentangled structure.

**Weak Supervision Label Model** The purpose of the label model is to encode relationships between the LFs  $\lambda_i$  and the latent label  $y$ , enabling us to produce an informed estimate of  $y$  from the LF outputs. The model is usually a factor graph with potentials  $\phi_j(\lambda_j(x), y)$  and  $\phi_{j,k}(\lambda_j(x), \lambda_k(x))$  capturing the degree of agreement between  $\lambda_j$  and  $y$  or correlations between  $\lambda_j$  and  $\lambda_k$ . For example, we set  $\phi_j(\lambda_j, y) \triangleq \mathbb{1}\{\lambda_j = y\}$  as in related work. These potentials  $\phi_j$  are associated with accuracy parameters  $\theta_j$ .

Once we obtain estimates of  $\theta_j$ , we can predict  $y$  from the

LFs  $\lambda$  using the function  $L_\theta(\lambda) : \{0, 1, \dots, C\}^m \rightarrow [0, 1]^C$ ,

$$L_\theta(\lambda)_k = \frac{\exp(\sum_{j=1}^m \theta_j \phi_j(\lambda_j(x), k))}{\sum_{\tilde{y} \in \mathcal{Y}} \exp(\sum_{j=1}^m \theta_j \phi_j(\lambda_j(x), \tilde{y}))}, \quad (3)$$

for  $k = 1, \dots, C$ . This is a softmax over the weighted votes of all LFs, a conventional approach which derived from the factor graph introduced in Ratner et al. (2016). Note that related work only models the LF outputs to learn  $\theta$ , ignoring additional information in the features  $x$ .

However, the structure of the input data is crucial to our fusion. For this reason, we use a modified label model predictor in the spirit of Cachay et al. (2021). It generates *local* accuracy parameters—sample-dependent parameters encoding how accurate each  $\lambda_i$  is estimated to be—via an accuracy parameter encoder  $A(x) : \mathbb{R}^d \rightarrow \mathbb{R}_+^m$ . This variant is given by:

$$L_{A_\theta}(\lambda)_k = \frac{\exp(\sum_{j=1}^m A(x)_j \phi_j(\lambda_j(x), k))}{\sum_{\tilde{y} \in \mathcal{Y}} \exp(\sum_{j=1}^m A(x)_j \phi_j(\lambda_j(x), \tilde{y}))}, \quad (4)$$

for  $k = 1, \dots, C$ . This is again a softmax over the LF votes by class, weighted by the accuracy encoder output. Note that while  $A(x)$  allows for finer-grained adjustments of the label estimate  $\hat{Y}$ , the estimate is still anchored in the votes of LFs which should represent strong domain knowledge.

**Learning the Label Model** The technical challenge of weak supervision is to learn the parameters of the label model (such as  $\theta_j$  above) without observing  $y$ . All existing approaches find parameters that (i) best explain the LF votes while (ii) satisfying conditionally independent relationships (Ratner et al., 2016, 2019; Fu et al., 2020). The features  $x$  are ignored; it is assumed that all information about  $y$  is present in the LF outputs.

We instead promote cooperation between our models by ensuring that *the best label model is the one which agrees with the discrete structure that the GAN can learn, and vice versa*. The intuition for this key notion is that as each of the generative and label models learn useful information from data, this information can—if aligned correctly—be shared to help teach the other model. To this end, note that in InfoGAN, the model  $Q$  is only applied to generated samples as the sampled variable  $b$  can be observed for generated images, but not for real images. Nonetheless,  $Q$  can be applied to the real-world samples to obtain a prediction of the latent  $b$ . Crucially, in the weak supervision setting we also observe the LF outputs, enabling us derive a label estimate for each real image:

$$L_{A_\theta}(\lambda) = \hat{Y},$$

which we can use to guide the structure corresponding to  $b$  and vice versa.

**Interface Models and Overall WSGAN Objective** We introduce the following *interface* models to map between the discrete  $b$  and label estimates. Let  $F_1 : [0, 1]^C \rightarrow [0, 1]^C$  and  $F_2 : [0, 1]^C \rightarrow [0, 1]^C$ . An effective choice for  $F_1$  and  $F_2$  are linear models with a softmax activation function.

To achieve agreement between the latent structure discovered by the GAN’s auxiliary model  $Q$  as well as by the label model  $L_{A_\theta}$  via the LFs, we introduce the following overall objective, ensuring that a mapping exists between the latent structures on the training data:

$$\min_{G, Q, F_1, F_2, A} \max_D IV(D, G, Q) \quad (5)$$

$$+ \beta \mathbb{E}_{x, \lambda \sim p_t(x, \lambda)} [l(F_1(Q(x)), L_A(\lambda)) + l(Q(x), F_2(L_A(\lambda)))],$$

where  $\beta$  is a trade-off parameter, and  $l$  again denotes an appropriate loss function such as the cross entropy. Pseudocode for the added loss term can be found in Algorithm 1 in the Appendix.

**Improving Alignment** Importantly, initializing the label model  $L_A$  with equal weights results in a strong baseline estimate of  $\hat{Y}$ , as LFs are built to be better than random. Similarly, as noted in Cachay et al. (2021), initializing the accuracy parameter encoder  $A(x)$  with random weights will also lead to a label estimate close to an equally-weighted vote. Initializing  $L_{A_\theta}$  in this way can therefore guide  $Q$  towards the discrete structure encoded in the LFs. To reinforce this behavior and to stabilize learning, we find that adding a decaying penalty term that encourages equal label model weights in early epochs—while not necessary to achieve good performance—almost always improves performance further. Let  $i \geq 0$  denote the current epoch. We propose to add the following linearly decaying penalty term for an encoder  $A$  that uses a sigmoid activation function:

$$\frac{C}{i \times \gamma + 1} \|A(x) - \bar{1} \times 0.5\|_2^2, \quad (6)$$

where  $\gamma$  is a decay parameter. In our experiments we set  $\gamma = 1.5$ .

Further, note that  $D, Q, A$  all encode images. In InfoGAN,  $Q$  and  $D$  generally share all convolutional layers but have distinct prediction heads. We let  $A$  share the same convolutional layers and detach the output from the computation graph before passing it to a small multilayer perceptron (MLP) followed by a sigmoid activation function. Thus, the WSGAN method only adds a small number of additional parameters compared to a basic GAN.

**Augmenting the Weak Supervision Pipeline with Synthetic Data** Given a WSGAN model trained according to Eq. 5, we can generate images via  $G$  to obtain unlabeled

synthetic samples  $\tilde{x}$ . To obtain pseudolabels for these images we have at least one and sometimes two options to generate pseudolabels. When LFs can be applied to synthetic images, we can obtain their votes  $\tilde{\lambda}$  and apply our WSGAN label model  $L_A(\tilde{\lambda})$ . However, in many practical applications of weak supervision, LFs are not applied to images directly, but rather to metadata or an auxiliary modality such as text (cf. Section 5). With WSGAN, we can obtain pseudolabels nonetheless via  $\hat{y} = F_1(Q(\tilde{x}))$  using the trained WSGAN components  $Q$  and  $F_1$ , in essence transferring knowledge from  $Q$  to the end model. Note that the quality of these synthetic pseudolabels hinges on the performance of  $Q$ , which can conceivably improve with the supply of weakly supervised as well as entirely unlabeled data.

## 4 Experiments

Our experiments on seven weakly supervised datasets show that the WSGAN approach is able to take advantage of the discrete structure it discovers in the images, leading to better performance compared to label models of prior work. Our results also indicate that weak supervision as used by WSGAN can improve image generation performance, as well as the quality of the auxiliary model which learns disentangled discrete structure. We will first describe the experimental setup and then discuss the results. Additional baselines comparing against direct combinations of weak supervision to improve generative modeling (and vice-versa) can be found in Appendix B.

### 4.1 Setup

**Datasets** Table 1 shows key characteristics of the datasets used in our experiments, including information about the different LF sets. We create the following weakly supervised image classification datasets:

- *CIFAR10*: We create two sets of LFs for two subsets of the data. One set uses the full training set of CIFAR10 (minus 300 samples held out for downstream validation), while the second is a random subset of 30,000 training images. For each of these two splits we generate two sets of synthetic LFs based on the true class label; one set of 20 LFs and an extended set of 40 LFs, resulting in a total of four CIFAR10 experiments. We create the synthetic unipolar LFs via the following procedure: for each LF we sample a class label, an error rate, and a propensity (i.e., the percentage of samples where the LF casts a vote, also referred to as coverage). Given the target label, we then sample true positives and false positives at random to achieve the desired LF accuracy and propensity.
- *DomainNet*: We follow [Mazzetto et al. \(2021a\)](#) and derive weak supervision sources for a multiclass classification task of the real images contained in the DomainNet

([Peng et al., 2019](#)) dataset. DomainNet contains 345 classes of images in 6 different domains<sup>1</sup>. First, we set our target domain to real images and select the 10 classes with the largest number of instances in this domain. As LFs, we then train classifiers using the selected classes within the remaining five domains, and apply them to the target domain of real images to obtain weak labels.

- *Animals with Attributes 2 (AwA2)*: We create two sets of LFs for the Animals with Attributes 2 (AwA2) ([Mazzetto et al., 2021a](#)) image classification dataset. AwA2 is an image dataset with known general attributes for each class, divided into 40 seen and 10 unseen classes. Following [Mazzetto et al. \(2021b,a\)](#), we train one-vs-rest attribute classifiers using the 40 seen classes. These classifiers are applied to the 10 unseen classes to produce weak attribute labels. At this stage, we discard attribute classifiers which perform worse than random. We create an 85%/5%/10% train/validation/test split of the 10 unseen classes which we use to define decision trees to produce weak labels on the bases of weak attribute predictions. We create the 29 unipolar LFs for AwA2-A by training 3 one-vs-rest decision trees per each of the 10 classes on 100 random samples from the training set. To create a slightly easier set, we create the 32 unipolar LFs used in AwA2-B by training 80 decision trees, retaining one random tree specializing in each class, and then selecting all remaining ones where validation accuracy is higher than 0.65.

To simplify the experiments, and to allow for easy reproducibility without requiring prohibitively extensive computations, we perform our experiments on small images and where necessary resize them to 32x32 pixels.

**Models** We provide implementation details and parameter settings for our models in Appendix A. We use the same hyperparameter settings in all experiments and evaluate the following proposed approaches:

- WSGAN-Encoder: Our proposed model, weighing LF votes of each sample by using the output of an *accuracy parameter encoder A* that takes in the image associated with the sample and returns a weight vector.
- WSGAN-Vector: Proposed model, but using a parameter vector to weigh LF votes in place of the encoder A.

We use a simple DCGAN ([Radford et al., 2015](#)) base encoder and decoder architecture (see Appendix A for details) for the proposed WSGAN approach as well as for the InfoGAN implementation. All networks are trained from scratch, and we only use pretrained classifiers to create LFs for the DomainNet and AwA2 datasets.

We provide performance comparisons to the following

<sup>1</sup>Real, painting, sketch, clipart, infograph, quickdraw.

Table 1: Datasets and labeling function (LF) characteristics used to evaluate the proposed WSGAN model. Acc denotes accuracy, while Coverage denotes the number of samples where the LF does not abstain.

Dataset	#Classes	#LFs	#Samples	Mean LF Acc	Min LF Acc	Max LF Acc	Mean Coverage
CIFAR10-A	10	20	49700	0.747	0.621	0.879	0.048
CIFAR10-B	10	40	49700	0.760	0.621	0.898	0.052
CIFAR10-C	10	20	30000	0.773	0.624	0.896	0.061
CIFAR10-D	10	40	30000	0.761	0.624	0.896	0.056
AwA2 -A	10	29	6726	0.504	0.053	0.850	0.104
AwA2 -B	10	32	6726	0.548	0.116	0.783	0.131
DomainNet	10	4	6369	0.493	0.416	0.684	1.000

Table 2: Average posterior accuracy of various label models on training samples with at least one LF vote. We highlight the best result in **blue** and the second best result in **bold**.

Dataset	MV	DawidSkene	MeTaL	FS	Snorkel	WSGAN-Vector	WSGAN-Encoder
CIFAR10-A	0.7623	<b>0.7776</b>	0.7511	0.7635	0.7566	<b>0.7780</b>	<b>0.7960</b>
CIFAR10-B	0.8305	<b>0.8609</b>	0.8128	0.8050	0.8123	0.8536	<b>0.8650</b>
CIFAR10-C	0.8268	<b>0.8501</b>	0.8063	0.8003	0.8073	<b>0.8497</b>	<b>0.8737</b>
CIFAR10-D	0.8647	<b>0.9020</b>	0.8454	0.8265	0.8485	0.8984	<b>0.9163</b>
AwA2 - A	0.6312	0.6068	0.6323	0.6146	0.6412	<b>0.6469</b>	<b>0.6809</b>
AwA2 - B	0.6232	0.5482	0.5819	0.6021	0.6045	<b>0.6453</b>	<b>0.6993</b>
DomainNet	0.6143	<b>0.6581</b>	0.4865	0.6354	0.5992	<b>0.6605</b>	0.6466

related label model approaches:<sup>2</sup>

- Snorkel (Ratner et al., 2016, 2020): a probabilistic graphical model that estimates LF parameters by maximizing the marginal likelihood using observed LFs.
- Dawid-Skene (Dawid & Skene, 1979): a model motivated by the crowdsourcing setting. The model, fit using expectation maximization, assumes that error statistics of sources are the same across classes and that errors are equiprobable independent of the true class.
- Snorkel MeTaL (Ratner et al., 2019): a Markov random field (MRF) model similar to Snorkel which uses a technique to complete the inverse covariance matrix of the MRF during model fitting, and also allows for modeling multi-task weak supervision.
- FlyingSquid (FS) (Fu et al., 2020): based on a label model similar to Snorkel, FS provides a closed form solution by augmenting it to set up a binary Ising model, enabling scalable model fitting.
- Majority Vote (MV): A standard scheme that uses the most popular LF output as the estimate of the true label.

**Evaluation Metrics** Label model performance is compared based on the accuracy of pseudo-labels the models

<sup>2</sup>Implementations available via WRENCH (Zhang et al., 2021)

achieve on the training data. To show the improvement in alignment of the auxiliary model  $Q(b|x)$ 's predictions of the discrete latent code  $b$  with the latent labels  $y$ , we track the Adjusted Rand Index (ARI) between the two during training. To compare the quality of generated images, we use the Fréchet Inception Distance (FID) which has been shown to be consistent with human judgments and to be more robust than related measures (Heusel et al., 2017). While FID is known to be biased as a function of the generator and number of generated samples  $N$  (Chong & Forsyth, 2020), the relative ordering in this paper is informative as we use the same generator and  $N$  for our model and InfoGAN.

## 4.2 Results

We will first discuss results comparing label model and image generation performance, before discussing the use of WSGAN for augmentation of the downstream classifier with synthetic samples. We repeat each experiment four times and average the results in our tables.

### 4.2.1 Label Model and Image Generation

**Label Model Performance** Table 2 shows a comparison of label model performance based on the accuracy of the posterior on the training data, without the use of any labeled data or validation sets. WSGAN-encoder largely outperforms al-

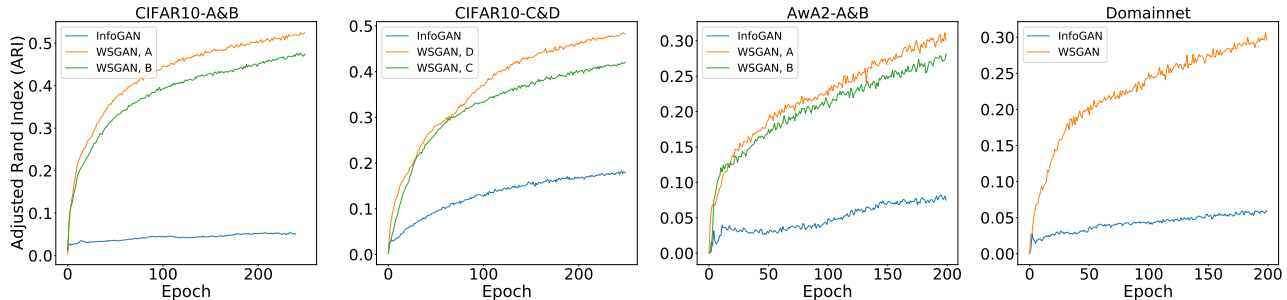


Figure 3: Adjusted Rand Index between  $y$  and  $Q(x)$ , i.e. a measurement of the similarity between the true class labels and the discrete code prediction by the GAN’s auxiliary model  $Q$ . The graphs show improved uncovering of the latent class structure by the  $Q$  of WSGAN.

Table 3: Image generation quality measured by average Fréchet Inception Distance (FID). The best scores for each dataset are highlighted in blue.

Dataset	InfoGAN	WSGAN-V	WSGAN-E
CIFAR10-A	33.64	<b>24.11</b>	26.0
CIFAR10-B	33.64	24.09	<b>23.78</b>
CIFAR10-C	28.93	25.7	<b>22.71</b>
CIFAR10-D	28.93	<b>21.97</b>	22.63
AwA2 - A	41.62	36.74	<b>34.71</b>
AwA2 - B	41.62	36.79	<b>34.52</b>
DomainNet	51.88	51.16	<b>45.6</b>

ternative label models, while the simpler WSGAN-vector model performs competitively as well. Not unexpectedly, the Dawid-Skene model performs quite well on the synthetic LFs of the CIFAR10 datasets, as the random errors of the LFs match the assumptions of the approach.

**Discrete Latent Code Comparison** Figure 3 shows the evolving ARI between the ground truth and the auxiliary model  $Q$ ’s prediction of the latent code on real data during model training. The figures show a large improvement in  $Q$ ’s ability discover the unobserved class label structure when comparing WSGAN to InfoGAN, which is expected as WSGAN can take advantage of the weak signals encoded in LFs, while InfoGAN is completely unsupervised.

**Image Generation Performance** Table 3 compares FID of generated images, suggesting that WSGAN models do take advantage of the weak supervision signal to improve  $Q$ , thereby improving the quality of generated images compared to an InfoGAN of the same architecture.

Table 4: Increase in test accuracy when augmenting downstream classifier training with 1,000 synthetic images and corresponding pseudo labels. Synthetic pseudolabels are obtained via  $F_1(Q(\tilde{x}))$ , LF pseudolabels via  $L_{A(\tilde{x})}(\lambda(\tilde{x}))$

Dataset	Synthetic Pseudolabels	LF Pseudolabels
CIFAR10-C	0.04%	-
CIFAR10-D	0.98%	-
AwA2 - A	0.88%	0.79%
AwA2 - B	2.4%	3.9%
DomainNet	2.31%	1.5%

#### 4.2.2 Synthetic Data Augmentation

We record the change in test accuracy for a ResNet-18 (He et al., 2016) end model when adding 1,000 synthetic WSGAN-encoder images  $\tilde{x}$  to augment each small dataset.

**Synthetic Images with Synthetic Pseudolabels** Without access to LF votes on fake images, we create synthetic pseudolabels  $F_1(Q(\tilde{x}))$ . The second column of Table 4 shows the increase in test accuracy, indicating that a modest increase of up to 2.4% was achieved. We do not observe larger increases in accuracy by adding more generated images. Figure 1 shows a small number of generated images along with their synthetic pseudolabel estimate. While  $F_1(Q(x))$  could conceivably be used as a downstream classifier, the choices of architecture are constrained as it shares convolutional layers with  $D$ .

**Synthetic Images with Labeling Function Votes** Here, we apply our LFs to the generated images to obtain LF votes  $\lambda(\tilde{x})$ . We obtain pseudolabels via the WSGAN label model  $L_{A(\tilde{x})}(\lambda(\tilde{x}))$ . The third column in Table 4 displays improvements in test accuracy up to 3.9%. We have to omit the CIFAR10 datasets for this experiment as the LFs are

simulated solely based on the true  $Y$  and not based on the images themselves.

**Synthetic Data Quality Checks** In addition to visually inspecting some of the generated samples, we recommend checking the class balance in the pseudolabels of synthetic images before adding them to a downstream training set, as mode collapse in a trained GAN can potentially be diagnosed this way. We were able to automatically discard some rare low quality sets of generated images.

## 5 Related Work

Here, we briefly review relevant work in weak supervision, generative modeling, and data augmentation via GANs.

**Programmatic Weak Supervision** Data programming (DP) (Ratner et al., 2016) is a popular weak supervision framework in which subject matter experts programmatically label data through multiple noisy sources of labels known as labeling functions (LFs). These LFs capture partial knowledge about an unobserved ground truth variable at better than random accuracy. In this paradigm, LF votes are combined to derive an estimate of the unobserved ground truth, which is then used to train an end model using a noise-aware loss function. DP has been successfully applied to various domains including medicine (Fries et al., 2019; Dunnmon et al., 2020; Eyuboglu et al., 2021) and industry applications (Ré et al., 2020; Bach et al., 2019).

Many works offer data programming label models with improved properties, e.g., extensions to multitask models (Ratner et al., 2019), better computational efficiency (Fu et al., 2020), exploiting small amounts of labels as in semi-supervised learning (Chen et al., 2021; Mazzetto et al., 2021a,b), end-to-end training (Cachay et al., 2021), interactive learning (Boecking et al., 2021), or extensions to structured prediction settings (Shin et al., 2022). See (Zhang et al., 2022) for a more detailed survey.

**Weak Supervision and Images** Our main focus is on applications of weak supervision to image data. On images, imperfect labels are often obtained from domain specific primitives and rules (Varma & Ré, 2018; Fries et al., 2019), rules defined on top of annotations by surrogate models (Varma & Ré, 2018; Chen et al., 2019; Hooper et al., 2021), and rules defined on meta-data (Li & Fei-Fei, 2010; Chen & Gupta, 2015; Izadinia et al., 2015; Denton et al., 2015; Boecking et al., 2021) or a second paired modality such as text (Joulin et al., 2016; Wang et al., 2017; Irvin et al., 2019; Saab et al., 2019; Dunnmon et al., 2020; Eyuboglu et al., 2021).

**Generative Models and Disentangled Representations** Among the numerous existing approaches to generative mod-

eling, in this work we focus on generative adversarial networks (GANs) (Goodfellow et al., 2014). We are particularly interested in work that aims to learn disentangled representations (Chen et al., 2016; Lin et al., 2020) that can align with class variables of interest. Chen et al. (2016) introduce InfoGAN, which learns interpretable latent codes. This is achieved by maximizing the mutual information between a fixed small subset of the GAN’s input variables and the generated observations. Gabbay & Hoshen (2020) present a unified formulation for class and content disentanglement as well as a new approach for class-supervised content disentanglement. Nie et al. (2020) study semi-supervised high-resolution disentanglement learning for the state-of-the-art StyleGAN architecture. A potential downside to modeling latent factors in generative models is a decrease in image quality of generated samples that has been noted when disentanglement terms are added (Burgess et al., 2018; Khruikov et al., 2021).

Prior work has studied how to integrate additional information into GAN training, in particular ground truth class labels (Mirza & Osindero, 2014; Odena et al., 2017; Brock et al., 2019). However, in the weak supervision setting, the imperfect labels and noise in any derived label estimate present large hurdles to similar conditional modeling. Some prior work uses other weak forms of supervision to aid specific aspects of generative modeling. For example, Chen & Batmanghelich (2020) propose learning disentangled representation using user-provided ground-truth pairs. Yet, prior work does not fuse generic weak supervision frameworks and generative models, and so are limited to one-off techniques to solely improve generative models.

**Using GANs for Data Augmentation** An exciting application of GANs is to generate additional samples for supervised model training. The challenge is to produce sufficiently high-quality samples. For example, Abbas et al. (2021) use a conditional GAN to generate synthetic images of tomato plant leaves for a disease detection task. GANs for data augmentation are also popular in medical imaging (Yi et al., 2019; Motamed et al., 2021; Hu et al., 2019). For example, Hu et al. (2019) use an InfoGAN-like model to learn cell-level representations in histopathology, Motamed et al. (2021) augment radiology data, and Pascual et al. (2019) generate synthetic epileptic brain activities.

## 6 Conclusion

We studied the question of how to build an interface between two powerful techniques that operate in the absence of labeled data: generative modeling and weak supervision. Our fusion of the two, a weakly supervised GAN (WSGAN), uses an interface that aligns structures discovered in their constituent models. It lead to three improvements: first, better quality pseudolabels compared to weak supervision

alone, boosting downstream performance. Second, improvement in the quality of the generative model samples. Third, it enabled the use of such samples for data augmentation, further improving downstream model performance without additional burden on users.

Our proposed approach leads to several exciting directions for future work. We plan to extend the generative model component in the fused model to progressively grown GANs (Karras et al., 2018) to handle larger and higher fidelity images. We are also interested in other modalities, exploiting for instance generative models for graphs and time series. Finally, motivated by the performance of WSGAN, we seek to extend the underlying notion of interfaces between models to a variety of other pairs of models.

## References

- Abbas, A., Jain, S., Gour, M., and Vankudothu, S. Tomato plant disease detection using transfer learning with c-gan synthetic images. *Computers and Electronics in Agriculture*, 187:106279, 2021.
- Bach, S. H., Rodriguez, D., Liu, Y., Luo, C., Shao, H., Xia, C., Sen, S., Ratner, A., Hancock, B., Alborzi, H., et al. Snorkel drybell: A case study in deploying weak supervision at industrial scale. In *Proceedings of the 2019 International Conference on Management of Data*, pp. 362–375, 2019.
- Barratt, S. and Sharma, R. A note on the inception score. *arXiv preprint arXiv:1801.01973*, 2018.
- Boecking, B., Neiswanger, W., Xing, E., and Dubrawski, A. Interactive weak supervision: Learning useful heuristics for data labeling. In *International Conference on Learning Representations*, 2021.
- Borji, A. Pros and cons of gan evaluation measures. *Computer Vision and Image Understanding*, 179:41–65, 2019.
- Brock, A., Donahue, J., and Simonyan, K. Large scale GAN training for high fidelity natural image synthesis. In *International Conference on Learning Representations*, 2019.
- Burgess, C. P., Higgins, I., Pal, A., Matthey, L., Watters, N., Desjardins, G., and Lerchner, A. Understanding disentangling in  $\beta$ -vae. *arXiv preprint arXiv:1804.03599*, 2018.
- Cachay, S. R., Boecking, B., and Dubrawski, A. End-to-end weak supervision. *Thirty-fifth Conference on Neural Information Processing Systems (NeurIPS)*, 2021.
- Chen, J. and Batmanghelich, K. Weakly supervised disentanglement by pairwise similarities. In *Proceedings of the AAAI Conference on Artificial Intelligence*, volume 34, pp. 3495–3502, 2020.
- Chen, M., Cohen-Wang, B., Mussmann, S., Sala, F., and Ré, C. Comparing the value of labeled and unlabeled data in method-of-moments latent variable estimation. In *International Conference on Artificial Intelligence and Statistics*, pp. 3286–3294. PMLR, 2021.
- Chen, V., Wu, S., Ratner, A. J., Weng, J., and Ré, C. Slice-based learning: A programming model for residual learning in critical data slices. In *Advances in Neural Information Processing Systems*, pp. 9392–9402, 2019.
- Chen, X. and Gupta, A. Webly supervised learning of convolutional networks. In *Proceedings of the IEEE International Conference on Computer Vision*, pp. 1431–1439, 2015.
- Chen, X., Duan, Y., Houthoofd, R., Schulman, J., Sutskever, I., and Abbeel, P. Infogan: interpretable representation learning by information maximizing generative adversarial nets. In *Neural Information Processing Systems (NIPS)*, 2016.
- Chong, M. J. and Forsyth, D. Effectively unbiased fid and inception score and where to find them. In *Proceedings of the IEEE/CVF conference on computer vision and pattern recognition*, pp. 6070–6079, 2020.
- Dawid, A. P. and Skene, A. M. Maximum likelihood estimation of observer error-rates using the em algorithm. *Journal of the Royal Statistical Society: Series C (Applied Statistics)*, 28(1):20–28, 1979.
- Dehghani, M., Zamani, H., Severyn, A., Kamps, J., and Croft, W. B. Neural ranking models with weak supervision. In *Proceedings of the 40th International ACM SIGIR Conference on Research and Development in Information Retrieval*, pp. 65–74. Association for Computing Machinery, 2017.
- Denton, E., Weston, J., Paluri, M., Bourdev, L., and Fergus, R. User conditional hashtag prediction for images. In *Proceedings of the 21th ACM SIGKDD international conference on knowledge discovery and data mining*, pp. 1731–1740, 2015.
- Dunnmon, J. A., Ratner, A. J., Saab, K., Khandwala, N., Markert, M., Sagreiya, H., Goldman, R., Lee-Messer, C., Lungren, M. P., Rubin, D. L., and Re, C. Cross-modal data programming enables rapid medical machine learning. *Patterns*, 1(2):100019, 2020.
- Eyuboglu, S., Angus, G., Patel, B. N., Pareek, A., Davidzon, G., Long, J., Dunnmon, J., and Lungren, M. P. Multi-task

- weak supervision enables anatomically-resolved abnormality detection in whole-body fdg-pet/ct. *Nature communications*, 12(1):1–15, 2021.
- Fries, J. A., Varma, P., Chen, V. S., Xiao, K., Tejeda, H., Saha, P., Dunnmon, J., Chubb, H., Maskatia, S., Fiterau, M., et al. Weakly supervised classification of aortic valve malformations using unlabeled cardiac mri sequences. *Nature Communications*, 10(1):1–10, 2019.
- Fu, D. Y., Chen, M. F., Sala, F., Hooper, S. M., Fatahalian, K., and Ré, C. Fast and three-riuous: Speeding up weak supervision with triplet methods, 2020.
- Gabbay, A. and Hoshen, Y. Demystifying inter-class disentanglement. In *International Conference on Learning Representations*, 2020.
- Goodfellow, I. J., Pouget-Abadie, J., Mirza, M., Xu, B., Warde-Farley, D., Ozair, S., Courville, A., and Bengio, Y. Generative adversarial nets. In *Proceedings of the 27th International Conference on Neural Information Processing Systems - Volume 2, NIPS’14*, pp. 2672–2680, 2014.
- He, K., Zhang, X., Ren, S., and Sun, J. Deep residual learning for image recognition. In *Proceedings of the IEEE Conference on Computer Vision and Pattern Recognition*, pp. 770–778, 2016.
- Heusel, M., Ramsauer, H., Unterthiner, T., Nessler, B., and Hochreiter, S. Gans trained by a two time-scale update rule converge to a local nash equilibrium. *Advances in neural information processing systems*, 30, 2017.
- Higgins, I., Amos, D., Pfau, D., Racaniere, S., Matthey, L., Rezende, D., and Lerchner, A. Towards a definition of disentangled representations. *arXiv preprint arXiv:1812.02230*, 2018.
- Hooper, S., Wornow, M., Seah, Y. H., Kellman, P., Xue, H., Sala, F., Langlotz, C., and Ré, C. Cut out the annotator, keep the cutout: better segmentation with weak supervision. *International Conference on Learning Representations (ICLR)*, 2021.
- Hu, B., Tang, Y., Chang, E. I. C., Fan, Y., Lai, M., and Xu, Y. Unsupervised learning for cell-level visual representation in histopathology images with generative adversarial networks. *IEEE Journal of Biomedical and Health Informatics*, 23(3):1316–1328, 2019. doi: 10.1109/JBHI.2018.2852639.
- Irvin, J., Rajpurkar, P., Ko, M., Yu, Y., Ciurea-Ilcus, S., Chute, C., Marklund, H., Haghgoo, B., Ball, R., Shpan-skaya, K., et al. Chexpert: A large chest radiograph dataset with uncertainty labels and expert comparison. In *Proceedings of the AAAI conference on artificial intelligence*, volume 33, pp. 590–597, 2019.
- Izadinia, H., Russell, B. C., Farhadi, A., Hoffman, M. D., and Hertzmann, A. Deep classifiers from image tags in the wild. In *Proceedings of the 2015 Workshop on Community-Organized Multimodal Mining: Opportunities for Novel Solutions*, pp. 13–18, 2015.
- Joulin, A., Van Der Maaten, L., Jabri, A., and Vasilache, N. Learning visual features from large weakly supervised data. In *European Conference on Computer Vision*, pp. 67–84. Springer, 2016.
- Karras, T., Aila, T., Laine, S., and Lehtinen, J. Progressive growing of gans for improved quality, stability, and variation. In *International Conference on Learning Representations*, 2018.
- Khrulkov, V., Mirvakhobova, L., Oseledets, I., and Babenko, A. Disentangled representations from non-disentangled models. *arXiv preprint arXiv:2102.06204*, 2021.
- Lang, H. and Poon, H. Self-supervised self-supervision by combining deep learning and probabilistic logic. In *In Proceedings of the Thirty Fifth Annual Meeting of the Association for the Advancement of Artificial Intelligence (AAAI)*, 2021.
- Li, L.-J. and Fei-Fei, L. Optimol: automatic online picture collection via incremental model learning. *International journal of computer vision*, 88(2):147–168, 2010.
- Lin, Z., Thekumparampil, K., Fanti, G., and Oh, S. Infogancr and modelcentrality: Self-supervised model training and selection for disentangling gans. In *International Conference on Machine Learning*, pp. 6127–6139. PMLR, 2020.
- Locatello, F., Abbati, G., Rainforth, T., Bauer, S., Schölkopf, B., and Bachem, O. On the fairness of disentangled representations. *arXiv preprint arXiv:1905.13662*, 2019.
- Mazzeo, A., Cousins, C., Sam, D., Bach, S. H., and Upfal, E. Adversarial multi class learning under weak supervision with performance guarantees. In *International Conference on Machine Learning*, pp. 7534–7543. PMLR, 2021a.
- Mazzeo, A., Sam, D., Park, A., Upfal, E., and Bach, S. Semi-supervised aggregation of dependent weak supervision sources with performance guarantees. In *International Conference on Artificial Intelligence and Statistics*, pp. 3196–3204. PMLR, 2021b.
- Mirza, M. and Osindero, S. Conditional generative adversarial nets. *arXiv preprint arXiv:1411.1784*, 2014.
- Motamed, S., Rogalla, P., and Khalvati, F. Data augmentation using generative adversarial networks (gans) for

- gan-based detection of pneumonia and covid-19 in chest x-ray images. *Informatics in Medicine Unlocked*, 27: 100779, 2021. ISSN 2352-9148. doi: <https://doi.org/10.1016/j.imu.2021.100779>.
- Nie, W., Karras, T., Garg, A., Debnath, S., Patney, A., Patel, A., and Anandkumar, A. Semi-supervised stylegan for disentanglement learning. In *International Conference on Machine Learning*, pp. 7360–7369. PMLR, 2020.
- Odena, A., Olah, C., and Shlens, J. Conditional image synthesis with auxiliary classifier gans. In *International conference on machine learning*, pp. 2642–2651. PMLR, 2017.
- Pascual, D., Aminifar, A., Atienza, D., Ryvlin, P., and Wattenhofer, R. Synthetic epileptic brain activities using gans. *Machine Learning for Health (MLAH) at NeurIPS*, 2019.
- Peng, X., Bai, Q., Xia, X., Huang, Z., Saenko, K., and Wang, B. Moment matching for multi-source domain adaptation. In *Proceedings of the IEEE/CVF International Conference on Computer Vision*, pp. 1406–1415, 2019.
- Radford, A., Metz, L., and Chintala, S. Unsupervised representation learning with deep convolutional generative adversarial networks. *arXiv preprint arXiv:1511.06434*, 2015.
- Ratner, A., Hancock, B., Dunnmon, J., Sala, F., Pandey, S., and Ré, C. Training complex models with multi-task weak supervision. In *Proceedings of the AAAI Conference on Artificial Intelligence*, volume 33, pp. 4763–4771, 2019.
- Ratner, A., Bach, S. H., Ehrenberg, H., Fries, J., Wu, S., and Ré, C. Snorkel: Rapid training data creation with weak supervision. *The VLDB Journal*, 29(2):709–730, 2020.
- Ratner, A. J., De Sa, C. M., Wu, S., Selsam, D., and Ré, C. Data programming: Creating large training sets, quickly. In *Advances in Neural Information Processing Systems*, pp. 3567–3575, 2016.
- Ré, C., Niu, F., Gudipati, P., and Srisuwananukorn, C. Over-ton: A data system for monitoring and improving machine-learned products. In *Proceedings of the 10th Annual Conference on Innovative Data Systems Research*, 2020.
- Riedel, S., Yao, L., and McCallum, A. Modeling relations and their mentions without labeled text. In *Joint European Conference on Machine Learning and Knowledge Discovery in Databases*, pp. 148–163. Springer, 2010.
- Saab, K., Dunnmon, J., Goldman, R., Ratner, A., Sagreiya, H., Ré, C., and Rubin, D. Doubly weak supervision of deep learning models for head ct. In *International Conference on Medical Image Computing and Computer-Assisted Intervention*, pp. 811–819. Springer, 2019.
- Salimans, T., Goodfellow, I., Zaremba, W., Cheung, V., Radford, A., and Chen, X. Improved techniques for training gans. *Advances in neural information processing systems*, 29:2234–2242, 2016.
- Shin, C., Li, W., Vishwakarma, H., Roberts, N., and Sala, F. Universalizing weak supervision. *International Conference on Learning Representations (ICLR)*, 2022.
- Varma, P. and Ré, C. Snuba: automating weak supervision to label training data. *Proceedings of the VLDB Endowment*, 12(3):223–236, 2018.
- Wang, X., Peng, Y., Lu, L., Lu, Z., Bagheri, M., and Summers, R. M. Chestx-ray8: Hospital-scale chest x-ray database and benchmarks on weakly-supervised classification and localization of common thorax diseases. In *Proceedings of the IEEE conference on computer vision and pattern recognition*, pp. 2097–2106, 2017.
- Yi, X., Walia, E., and Babyn, P. Generative adversarial network in medical imaging: A review. *Medical image analysis*, 58:101552, 2019.
- Zhang, J., Yu, Y., Li, Y., Wang, Y., Yang, Y., Yang, M., and Ratner, A. Wrench: A comprehensive benchmark for weak supervision. In *Thirty-fifth Conference on Neural Information Processing Systems Datasets and Benchmarks Track (Round 2)*, 2021.
- Zhang, J., Hsieh, C.-Y., Yu, Y., Zhang, C., and Ratner, A. A survey on programmatic weak supervision, 2022.

---

**Algorithm 1** Pseudocode for the proposed WSGAN loss term which is added to the basic InfoGAN loss. Input images and LFs are assumed to be filtered to only contain samples with at least 1 non-abstaining LF vote.

---

```

input: Batch of real images  $X$  and one-hot encoded LFs  $\Lambda$ , label model  $L$ , networks  $Q, A, F_1, F_2$ , WSGAN mode  $m$ ,
number of classes  $C$ , current epoch  $i$ ,  $\gamma$  decay parameter.
 $\hat{b}, Z = Q(X)$  # get predicted code and image features  $Z$ 
if  $m == \text{"vector"}$ :
     $\theta = A_\theta()$  # WSGAN-vector: get weight vector.
else:
     $\theta = A_\theta(Z.detach())$  # WSGAN-encoder: predict weights using image features  $Z$ .
 $\hat{y} = L(\Lambda, \theta)$  # Get label estimate from labelmodel using weights  $\theta$ .
# Compute cross-entropy losses
 $loss = cecoss(F_1(\hat{b}), \hat{y}.detach())$ 
 $loss += cecoss(F_2(\hat{y}), \hat{b}.detach())$ 
 $loss += C/(i \times \gamma + 1)mse(\theta, \bar{1} \times 0.5)$  # add decaying loss keeping weights uniform.
return  $loss$ 

```

---

## A Implementation Details

**Models** *Generator  $G$ , Discriminator  $D$ , and auxilliary model  $Q$* : Figures 5 and 4 show the simple DCGAN (Radford et al., 2015) generator and discriminator architectures that we use in our experiments. As mentioned in the main paper, in InfoGAN  $Q$  and  $D$  are neural networks that generally share all convolutional layers, with a final fully connected layer to output predictions. We follow the same structure in our experiments. We set the dimension of the noise variable  $z$  to 100, and of  $b$  equal to the number of classes. We sample  $z$  from a normal distribution and  $b$  from a uniform discrete distribution.

*Accuracy Encoder  $A$* : For WSGAN-Vector,  $A$  is simply a parameter vector of the same length as the number of labeling functions. For WSGAN-Encoder, we use image features obtained from the shared convolutional layers of  $Q, D$ , which we detach from the computational graph before passing them on to an MLP prediction head. For images with  $32 \times 32$  pixels, the feature vector obtained from the shared convolutional layers is of size  $512 * 16$ . The MLP head of  $A$  is set to have three hidden layers of size (256, 128, 64), with ReLU activations, and an output layer the size of the number of labeling functions followed by a sigmoid function.

*Mappings  $F_1, F_2$* : We set  $F_1, F_2$  to each be simple linear models with a softmax at the output, and set the input and output size of each to the number of classes.

**(WS)GAN Training** We use the same hyperparameter settings for all datasets. We train all GANs for a maximum of 200 epochs. We use a batch size of 16 and find that this lower batch size leads to fewer collapses of the generator. We also conducted ablation experiments with a batch size of 8 and 32 and found no significant difference in FID image generation quality or pseudolabel accuracy. For WSGAN, we use four optimizers, one for each of the different loss terms: discriminator training, generator training, the Info loss term, and the WSGAN loss term. We use Adam for all optimizers and set the learning rates as follows:  $4 \times 10^{-4}$  for  $D$ ,  $1 \times 10^{-4}$  for  $G$ ,  $1 \times 10^{-4}$  for the info loss term, and  $8 \times 10^{-5}$  for the WSGAN loss term. We follow the same settings for InfoGAN training for the components shared with WSGAN.

We find that deploying discriminator label flipping (randomly calling a tiny percentage of real samples fake and vice versa) and label smoothing (adding small amounts of noise to the real target of 1.0 and fake target of 0.0) stabilizes and improves GAN training.

**Endmodel Training** We train a ResNet-18 (He et al., 2016) for 100 epochs on all datasets, using Adam and a learning rate scheduler. The learning rate scheduler uses a small validation set to make adjustments to the learning rate.

**Image Augmentation** We use the following random image augmentation functions during GAN and endmodel training: random crop and resize (cropping out a maximum height/width of 13%), random sharpness adjustment ( $p = 0.2$ ), random color jitter, and random Gaussian blur ( $p = 0.1$ ).

Layer (type:depth-idx)	Output Shape	Param #
InfoDCDiscriminator	--	--
└Sequential: 1-1	[16, 512, 4, 4]	--
└└Conv2d: 2-1	[16, 64, 32, 32]	1,792
└└└LeakyReLU: 2-2	[16, 64, 32, 32]	--
└└└Conv2d: 2-3	[16, 64, 16, 16]	65,600
└└└└LeakyReLU: 2-4	[16, 64, 16, 16]	--
└└└└Conv2d: 2-5	[16, 128, 16, 16]	73,856
└└└└└LeakyReLU: 2-6	[16, 128, 16, 16]	--
└└└└└Conv2d: 2-7	[16, 128, 8, 8]	262,272
└└└└└└LeakyReLU: 2-8	[16, 128, 8, 8]	--
└└└└└└Conv2d: 2-9	[16, 256, 8, 8]	295,168
└└└└└└└LeakyReLU: 2-10	[16, 256, 8, 8]	--
└└└└└└└Conv2d: 2-11	[16, 256, 4, 4]	1,048,832
└└└└└└└└LeakyReLU: 2-12	[16, 256, 4, 4]	--
└└└└└└└└Conv2d: 2-13	[16, 512, 4, 4]	1,180,160
└└└└└└└└└LeakyReLU: 2-14	[16, 512, 4, 4]	--
└└└└└└└└└Dropout: 2-15	[16, 512, 4, 4]	--
└Sequential: 1-2	[16, 1, 1, 1]	--
└└Conv2d: 2-16	[16, 1, 1, 1]	8,192

Figure 4: The DCGAN discriminator architecture used in our experiments.

Layer (type:depth-idx)	Output Shape	Param #
DCGeneratorThree	--	--
└Linear: 1-1	--	2
└Sequential: 1-2	[16, 3, 32, 32]	--
└└ConvTranspose2d: 2-1	[16, 512, 4, 4]	901,632
└└└BatchNorm2d: 2-2	[16, 512, 4, 4]	1,024
└└└ReLU: 2-3	[16, 512, 4, 4]	--
└└└ConvTranspose2d: 2-4	[16, 256, 8, 8]	2,097,408
└└└└BatchNorm2d: 2-5	[16, 256, 8, 8]	512
└└└└ReLU: 2-6	[16, 256, 8, 8]	--
└└└└ConvTranspose2d: 2-7	[16, 128, 16, 16]	524,416
└└└└└BatchNorm2d: 2-8	[16, 128, 16, 16]	256
└└└└└ReLU: 2-9	[16, 128, 16, 16]	--
└└└└└ConvTranspose2d: 2-10	[16, 64, 32, 32]	131,136
└└└└└└BatchNorm2d: 2-11	[16, 64, 32, 32]	128
└└└└└└ReLU: 2-12	[16, 64, 32, 32]	--
└└└└└└ConvTranspose2d: 2-13	[16, 3, 32, 32]	1,731
└└└└└└└Tanh: 2-14	[16, 3, 32, 32]	--

Figure 5: The DCGAN generator architecture used in our experiments.

Table 5: A comparison to using an ACGAN with pseudolabels. Image generation quality is measured by average Fréchet Inception Distance (FID). The best scores for each dataset are highlighted in **blue**.

Dataset	InfoGAN	ACGAN	ACGAN (crisp)	WSGAN-V	WSGAN-E
CIFAR10-A	33.64	36.53	26.61	<b>24.11</b>	26.0
CIFAR10-B	33.64	36.81	45.1	24.09	<b>23.78</b>
CIFAR10-C	28.93	79.15	25.53	25.7	<b>22.71</b>
CIFAR10-D	28.93	80.43	33.05	<b>21.97</b>	22.63
AwA2 - A	41.62	51.32	47.21	36.74	<b>34.71</b>
AwA2 - B	41.62	53.73	50.03	36.79	<b>34.52</b>
DomainNet	51.88	61.96	47.32	51.16	<b>45.6</b>

## B Additional Baselines

We compare against two additional baselines. First, we train a generative model that is conditioned on pseudolabel information with the aim of improving image generation performance; we use pseudolabels provided by established weak-supervision label models in this role. Second, we use a basic generative model to produce synthetic samples that augment a downstream classifier (with weak labels provided by outputs of weak supervision sources applied to the synthetic images). These two baselines represent the straightforward way to use weak supervision to improve generative modeling (and vice-versa). We observe that such naive combinations struggle compared to our proposed approach, further motivating the importance of the interface in WSGAN.

### B.1 Image Generation with Pseudolabels

As an additional GAN baseline to our proposed WSGAN, we slightly adapt an Auxiliary Classifier Generative Adversarial Network (ACGAN) (Odena et al., 2017) to condition it on pseudolabels. The ACGAN is run on all data, but the auxiliary loss on real data with pseudolabels is only used for samples where at least one labeling function does not abstain. We create two versions: (1) using probabilistic pseudolabels with a soft cross-entropy loss, and (2) another using *hard/crisp* labels with a cross-entropy loss. To provide the strongest possible baseline in this experiment, we obtain the pseudolabels via the Dawid-Skene label model as it attains the best performance on average over all datasets compared to other related label models. Results are provided in Table 5, showing that this baseline approach is frequently unable to overcome the noise in the pseudolabels to improve over the InfoGAN results, and that it does not perform better than WSGAN with an encoder. Furthermore, it was much more difficult to successfully fit this approach to data and many runs had to be discarded as the quality of the generator collapsed early during training.

### B.2 Data Augmentation for Downstream Classification with Synthetic Images

In this experiment, we augment the training set for a downstream classifier with synthetic images. As baselines, we generate synthetic images  $\tilde{x}$  with an InfoGAN, and then apply the image labeling functions  $\lambda$  to the generated images to obtain LF votes  $\lambda(\tilde{x})$ .<sup>3</sup> Pseudolabels for the synthetic images are then obtained by fitting label models to the real training data and then applying the label models to the labeling function outputs on the synthetic data. Table 6 compares InfoGAN + Snorkel and InfoGAN + DawidSkene baselines to the improvements in test accuracy obtained by using WSGAN and shows that we were unable to obtain improvements in downstream accuracy with the baselines, possibly due to performance of the InfoGAN on these small datasets.

<sup>3</sup>We have to omit the CIFAR10 datasets for this experiment as the LFs are simulated solely based on the true class labels and sampled error rates and not based on the images themselves.

Table 6: Increase in test accuracy by augmenting the downstream classifier training data with 1,000 synthetic images and corresponding pseudo labels. Experiments are conducted on datasets where labeling functions can be applied to synthetic images.

Dataset	WSGAN	InfoGAN + Snorkel	InfoGAN + DawidSkene
AwA2 - A	0.79%	-0.63%	-1.26%
AwA2 - B	3.9%	-1.01%	-1.77%
DomainNet	1.5%	0.02%	-3.14%

Table 7: Weighted mean average precision of various label models on training samples with at least one LF vote. We highlight the best result in **blue** and the second best result in **bold**.

Dataset	MV	DawidSkene	MeTaL	FS	Snorkel	WSGAN-Vector	WSGAN-Encoder
CIFAR10-A	0.664	0.763	0.758	0.737	0.751	<b>0.780</b>	<b>0.825</b>
CIFAR10-B	0.788	0.896	0.889	0.876	0.878	<b>0.901</b>	<b>0.908</b>
CIFAR10-C	0.796	0.866	0.855	0.838	0.854	<b>0.878</b>	<b>0.912</b>
CIFAR10-D	0.880	<b>0.954</b>	0.942	0.924	0.940	0.950	<b>0.959</b>
AwA2 - A	0.616	0.661	0.653	0.627	0.653	<b>0.672</b>	<b>0.737</b>
AwA2 - B	0.591	0.652	0.662	0.642	0.668	<b>0.681</b>	<b>0.743</b>
DomainNet	0.599	<b>0.702</b>	0.630	0.654	0.621	0.679	<b>0.795</b>

### C Additional Metrics

We provide additional metrics for the label model comparisons shown in Table 2 in the main paper. Again, results are averaged over 4 random runs. Table 8 shows the weighted F1 score, an average over all classes weighted by the support of each class. Table 7 shows weighted mean average precision, a metric that summarizes the precision-recall curve across all classes. We compute the average precision individually for each class (one vs. rest) and then aggregate the scores by summing them weighted by the support of each class to produce the weighted mean average precision score.

Table 8: Weighted F1 score of various label models on training samples with at least one LF vote. The F1 is computed separately for each class and then averaged weighted by the support of each class. We highlight the best result in **blue** and the second best result in **bold**.

Dataset	MV	DawidSkene	MeTaL	FS	Snorkel	WSGAN-Vector	WSGAN-Encoder
CIFAR10-A	0.726	<b>0.741</b>	0.723	0.713	0.718	<b>0.738</b>	<b>0.759</b>
CIFAR10-B	0.809	<b>0.839</b>	0.791	0.784	0.781	0.834	<b>0.844</b>
CIFAR10-C	0.824	<b>0.850</b>	0.797	0.796	0.798	<b>0.851</b>	<b>0.872</b>
CIFAR10-D	0.864	<b>0.901</b>	0.843	0.825	0.839	<b>0.899</b>	<b>0.916</b>
AwA2 - A	0.641	<b>0.665</b>	0.620	0.619	0.636	0.6373	<b>0.684</b>
AwA2 - B	0.604	<b>0.661</b>	0.580	0.597	0.593	<b>0.664</b>	<b>0.672</b>
DomainNet	0.603	<b>0.655</b>	0.443	0.622	0.468	<b>0.654</b>	<b>0.634</b>